IEEE Access
Multidisciplinary | Rapid Review | Open Access Journal

Received August 23, 2019, accepted September 5, 2019, date of publication September 18, 2019, date of current version October 1, 2019.

Digital Object Identifier 10.1109/ACCESS.2019.2942148

A High Frequency Injection Technique With Modified Current Reconstruction for Low-Speed Sensorless Control of IPMSMs With a Single DC-Link Current Sensor

JING ZHAO, (Student Member, IEEE), SHAMSUDDEEN NALAKATH, (Member, IEEE), AND ALI EMADI, (Fellow, IEEE)

McMaster Institute for Automotive Research and Technology, McMaster University, Hamilton, ON L8P 0A6, Canada

Corresponding author: Jing Zhao (zhaoj98@mcmaster.ca)

This work was supported in part by the Canada Excellence Research Chairs (CERC) Program.

ABSTRACT This paper proposes a high frequency injection technique applied for low-speed sensorless control of interior permanent magnet synchronous machines (IPMSM) with a single dc-link current sensor. The three-phase currents, which can be reconstructed by the measurement of a dc-link current sensor, always suffer from the immeasurable regions. The most challenging problem exists in the low modulation region, where no phase current can be measured by the dc-link current sensor, and it is rarely solved without PWM modifications. This paper proposes a six-direction square wave high frequency injection method to extend the voltage vector to the measurable region to achieve the three-phase current reconstruction and saliency-based sensorless control without modifying the space vectors of the pulse width modulation (PWM). In addition, the paper comes up with a modified reconstruction scheme to reduce the reconstruction error and improve the accuracy of the position estimation. This low-speed sensorless strategy using a single dc-link current sensor is implemented in dSpace platform and the performance is evaluated by experiments.

INDEX TERMS Interior permanent magnet synchronous machines, dc-link current sensor, six direction square wave injection, sensorless control, current reconstruction.

I. INTRODUCTION

AC machines are employed in different applications, such as in household appliances, industrial equipment, and transportation, with the help of rapid development of digital processors and power electronics. Among AC machines, permanent magnet synchronous machines (PMSM) have the dominant status because of the benefit of the strong magnet field generated by the permanent magnets. Owing to its spatial saliency, interior PMSMs (IPMSMs) have more advantages in flux weakening operation and torque production [1], [2]. To realize high dynamic performance and control requirement, knowledge of the rotor position and the stator phase currents are essential. In a typical electric drive system, sensors are installed to capture the current and position information. However, the use of the sensors causes increases in the volume and expense of the system. As the solutions, position sensorless control [3]–[7] or single current sensor control [8], [9] has been investigated widely in the applications where the cost and size are the main concerns. Interestingly, the position sensorless control with a single current sensor has been gaining more attention as an approach to combine the benefits from these two techniques [10], [11].

For single current sensor control methods, the sensor on the dc-link has been the best option because of its convenience in installation and simplicity in reconstruction [12], [13]. In the dc-link current sensor control method, the dc-link current is sampled at different time instants during one switching period based on the active voltage vector applied to the machine. The main challenge in accurately reconstructing the phase currents from the dc-link current measurement comes from the existence of the dead time of PWM, A/D conversion time, and the settling time of the inverter [13]. Therefore, it requires that the active voltage vector should last at least a certain

The associate editor coordinating the review of this manuscript and approving it for publication was Zhuang Xu.

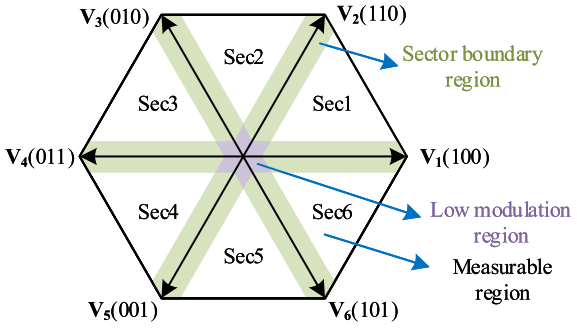

FIGURE 1. Spatial vector plane and immeasurable regions.

period to complete the current measurement so that the measured dc-link current can be associated with the active phase. Moreover, to reconstruct the three-phase currents, the dc-link current should be obtained at least twice in one cycle. In the sector boundary region, only one active voltage vector has sufficient interval to measure and to associate the corresponding currents whereas even a phase current is hardly detectable in the low modulation region. These two regions constitute the immeasurable region in the spatial vector plane, as shown in Fig. 1.

Various researches have been conducted and methods have been proposed such as observer-based methods [14]–[16] and PWM modification methods [17]–[19] to deal with this immeasurable problem. The observer-based method in [16] can accomplish desirable and comparable performance in medium- and high-speed operation by taking advantage of electromotive force (EMF), but not feasible at low-speed operation. The other method is to overcome the immeasurable region by modifying the PWM waveform. The most common method is the switching-state phase shift method (SSPS) [17]. This method maintains the duty cycle of each PWM via shifting the waveform to prolong the active switching state so that it provides sufficient duration for the dc-link current sensor to obtain the phase currents. This method creates asymmetrical PWM in the immeasurable region, thus increases the total harmonic distortion (THD). However, using this method to realize the position sensorless control with a single current sensor has deteriorating performance at low speed when high frequency (HF) signal is injected for the position estimation. [20] presents a saliency-based sensorless method with a single dc-link current sensor by injecting square wave voltage to d-axis, but the performance shown in the experiment is not up to the level as compared to the sensorless control with full current sensors. Reference [21] introduces an improved saliency-based method to reduce the reconstructed current error in the high frequency injection by using the current prediction on each current sampling instant. This scheme improves the sensorless control performance when applying high-frequency signals to derive the position information from the reconstructed current. However, this method relies on motor parameters and increases computational complexity.

This paper proposes a high frequency injection technique with modified current reconstruction for low-speed sensorless control of IPMSMs with a single dc-link current sensor. Compared with [20], the method can achieve better sensorless performance. Moreover, the method is relatively simply and easy to implement compared to [21]. The choice of the high frequency signal makes it possible for the reference voltage vector to avoid immeasurable region at low-speed operation without any PWM modification. This paper provides two options of high frequency square wave injection: β-axis injection and six-direction injection. β-axis injection method has the benefit of removing the filters. However, only phase B and phase C current are detectable from the dc-link current sensor, which causes an offset on reconstructed Phase A current due to the unaligned measurement problem. Also, the sensorless control by using this injection is dependent on the parameters of the motor. As the other option, six-direction square wave injection is not sensitive to the motor parameters and does not produce offset on the current reconstruction, but the filters are required. By comparison and analysis, the paper adopts six-direction square wave injection to realize low-speed operation with a dc-link current sensor. The paper also provides a modified current reconstruction scheme to minimize the reconstruction error from the different measurement instants of each phase current.

The paper is arranged as follows. Section II introduces the proposed high frequency injection method by analyzing the induced current equations. Section III presents the proposed current reconstruction method and saliency-based sensorless control in detail. The experimental results are given to verify the proposed low-speed sensorless control with a single dc-link current sensor in Section IV. The conclusion is drawn in Section V.

II. PROPOSED HIGH FREQUENCY VECTOR INJECTION TECHNIQUE

A. CONVENTIONAL RECONSTRUCTION METHOD

In the conventional full sensors control system, at least two current sensors are required to obtain two phase currents and the third phase current can be measured by a third sensor or calculated by the other two current values as:

$$i_a + i_b + i_c = 0 \tag{1}$$

The dc-link current sensor measures at the moments when the switches turn on and turn off according to the space vector modulation (SVM). For example, when the top switch of Phase A turns on and the top switches of Phase B and C turn off (Vector 1), the dc current goes through Phase A and it is equal to i_a, as shown in Fig. 2. According to seven-segment SVM scheme, two voltage vectors are used in one switching period to apply the reference voltage vector. That makes the current reconstruction possible by measuring dc-link current with only a single current sensor at two instants in a switching period. TABLE 1 provides the relationship between dc current samples and three-phase currents for each sector.

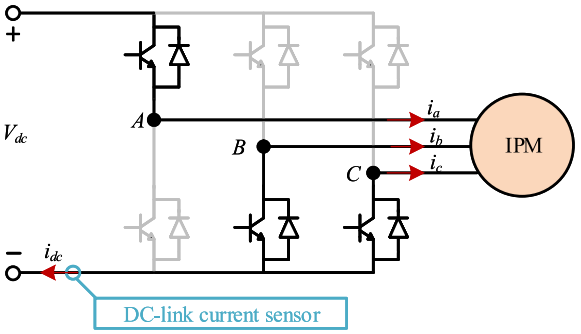

FIGURE 2. Principle of current sampling with dc-link current sensor.

TABLE 1. Three-phase current reconstruction method.

Sector	Switching State	First Current Sample	Second Current Sample
1	V_1, V_2	i_a	$-i_c$
2	V_3, V_2	i_b	$-i_c$
3	V_3, V_4	i_b	$-i_a$
4	V_5, V_4	i_c	$-i_a$
5	V_5, V_6	i_c	$-i_b$
6	V_1, V_6	i_a	$-i_b$

B. PROPOSED HIGH FREQUENCY SIGNAL INJECTION FOR CURRENT RECONSTRUCTION

When the reference voltage vector $\vec{V}_{ref}$ is in the sector boundary region, there is only one active voltage vector which has sufficient interval for the dc-link current sensor to capture the phase current. During medium- to high-speed operation, $\vec{V}_{ref}$ goes through the sector boundary region six times every one electrical cycle. The ratio of the immeasurable area to the measurable area increases with the reduction of the motor speed. When the speed is low enough, $\vec{V}_{ref}$ will enter into the low modulation region, where no phase current can be acquired from the dc-link current sensor. Therefore, high frequency injection is needed to force the $\vec{V}_{ref}$ outside the low modulation region. Meanwhile, HF is also used for the position sensorless control at standstill and low-speed operation. As a consequence, the determination of the HF is essential not only for the current reconstruction but also for the position sensorless control.

The mathematical model of IPM in $d-q$ rotational frame is written as:

$$\begin{bmatrix} v_d \\ v_q \end{bmatrix} = \begin{bmatrix} R_s & -\omega_e L_q \\ \omega_e L_d & R_s \end{bmatrix} \begin{bmatrix} i_d \\ i_q \end{bmatrix} + \begin{bmatrix} L_d & 0 \\ 0 & L_q \end{bmatrix} \cdot p \begin{bmatrix} i_d \\ i_q \end{bmatrix} + \begin{bmatrix} 0 \\ \omega_e \psi_m \end{bmatrix} \tag{2}$$

where R_s is denoted as the stator resistance, ψ_m is the flux linkage generated from the permanent magnet, and L_d and L_q are the inductances on d- and q- axes respectively.

When applying high frequency reference voltage to the machine, the derivative terms of currents dominate the voltage equations.

$$\begin{bmatrix} v_{d,h} \\ v_{q,h} \end{bmatrix} = \begin{bmatrix} L_d & 0 \\ 0 & L_q \end{bmatrix} \cdot p \begin{bmatrix} i_{d,h} \\ i_{q,h} \end{bmatrix} \tag{3}$$

where, $v_{d,h}$, $v_{q,h}$ are the injected voltage and $i_{d,h}$, $i_{q,h}$ are the induced currents by HF injection. The stationary frame equations can be expressed by using the transformation matrix, as

$$\begin{bmatrix} v_{\alpha,h} \\ v_{\beta,h} \end{bmatrix} = \mathbf{T_f} \begin{bmatrix} L_d & 0 \\ 0 & L_q \end{bmatrix} \mathbf{T_f}^{-1} \cdot p \begin{bmatrix} i_{\alpha,h} \\ i_{\beta,h} \end{bmatrix} \tag{4}$$

where,

$$\mathbf{T_f} = \begin{bmatrix} \cos(\theta_e) & -\sin(\theta_e) \\ \sin(\theta_e) & \cos(\theta_e) \end{bmatrix}$$

The voltage equation can be rewritten after simplifying and rearrangement, as

$$\begin{bmatrix} v_{\alpha,h} \\ v_{\beta,h} \end{bmatrix} = \begin{bmatrix} L + \Delta L\cos(2\theta_e) & \Delta L\sin(2\theta_e) \\ \Delta L\sin(2\theta_e) & L - \Delta L\cos(2\theta_e) \end{bmatrix} \cdot p \begin{bmatrix} i_{\alpha,h} \\ i_{\beta,h} \end{bmatrix} \tag{5}$$

where,

$$L = \frac{L_d + L_q}{2}, \Delta L = \frac{L_d - L_q}{2}$$

The derivative current can be shown as

$$p \begin{bmatrix} i_{\alpha,h} \\ i_{\beta,h} \end{bmatrix} = \frac{1}{L^2 - \Delta L^2} \mathbf{L_h} \begin{bmatrix} v_{\alpha,h} \\ v_{\beta,h} \end{bmatrix} \tag{6}$$

where,

$$\mathbf{L_h} = \begin{bmatrix} L + \Delta L\cos(2\theta_e) & \Delta L\sin(2\theta_e) \\ \Delta L\sin(2\theta_e) & L - \Delta L\cos(2\theta_e) \end{bmatrix}$$

1) PROPOSED β-AXIS SQUARE WAVE INJECTION

One of the HF options proposed in this paper is β-axis square wave injection. The frequency of the injected square wave is set to half of the switching frequency, as shown in Fig. 3. With the help of β-axis square wave injection, $\vec{V}_{ref}$ has an extension on the magnitude and change in angle close to β-axis. Consequently, the reference voltage vector is limited in Sector 2 and Sector 5. The oscillation only exists on Phase B and C as observed in Fig. 4(a). For current reconstruction with a dc-link current sensor with β-axis square wave injection, the current measurement is always targeted on Phase B and C, and the current of Phase A is always calculated by the other two phase currents. Due to the fact that two measured currents are obtained at different instants, the reconstructed Phase A current results in an offset as shown in Fig. 4. Moreover, the offset of the reconstruction is also impacted by the offset of the dc-link current sensor.

The injected voltage can be expressed as:

$$\begin{bmatrix} v_{\alpha,h} \\ v_{\beta,h} \end{bmatrix} = \begin{bmatrix} 0 \\ (-1)^n V_h \end{bmatrix} \tag{7}$$

where, V_h is the magnitude of the injection voltage.

The derivative current can be expressed as the current difference between adjacent samples, as

$$\begin{bmatrix} \Delta i_{\alpha,h} \\ \Delta i_{\beta,h} \end{bmatrix} = \frac{(-1)^n V_h}{L^2 - \Delta L^2} \begin{bmatrix} \Delta L\sin(2\theta_e) \\ L - \Delta L\cos(2\theta_e) \end{bmatrix} \tag{8}$$

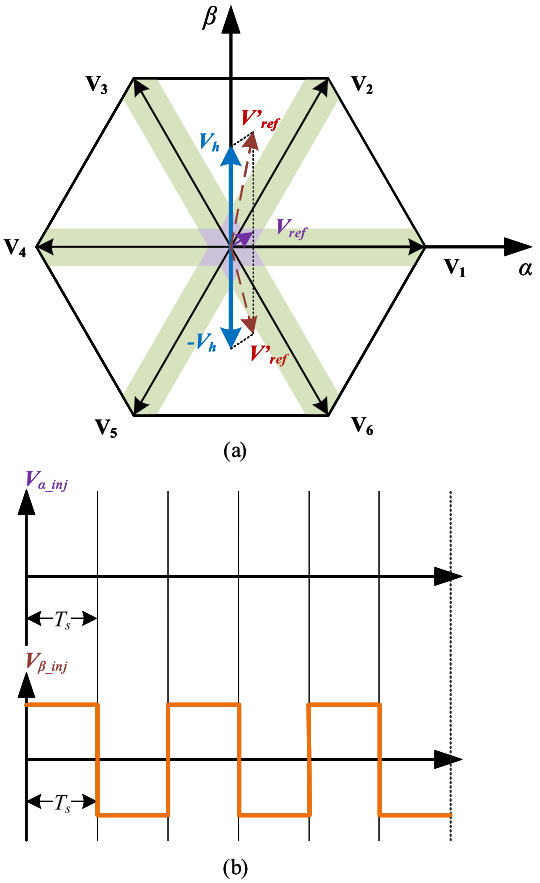

FIGURE 3. (a) Illustration of β-axis injection, (b) injection waveform in $\alpha - \beta$ frame.

So the position information exists in the envelope of the current difference between two switching period, as

$$\begin{bmatrix} \Delta i'_{\alpha,h} \\ \Delta i'_{\beta,h} \end{bmatrix} = \begin{bmatrix} I_2 sin(2\theta_e) \\ I_1 - I_2 \cos(2\theta_e) \end{bmatrix} \tag{9}$$

where,

$$I_1 = \frac{V_h L}{L^2 - \Delta L^2}, \quad I_2 = \frac{V_h \Delta L}{L^2 - \Delta L^2}$$

According to the current equation, this injection method is sensitive to the precision of the inductance parameters. Also, the injection only gives the excitation to Phase B and Phase C, which may cause the reconstruction of the three-phase current unbalanced and inaccurate.

2) PROPOSED SIX-DIRECTION SQUARE WAVE INJECTION

In order to make sure every voltage reference in each switching period is measurable, six-direction square wave injection method as shown in Fig. 5 is proposed in this paper. Instead of limiting the reference voltage vector in Sector 2 and 5 in the β-axis injection, this method rotates the $\overrightarrow{V}_{ref}$ to traverse each sector successively. Therefore, the current measurement involves all the three-phase currents, so that it can weaken the influence from the sensor offset.

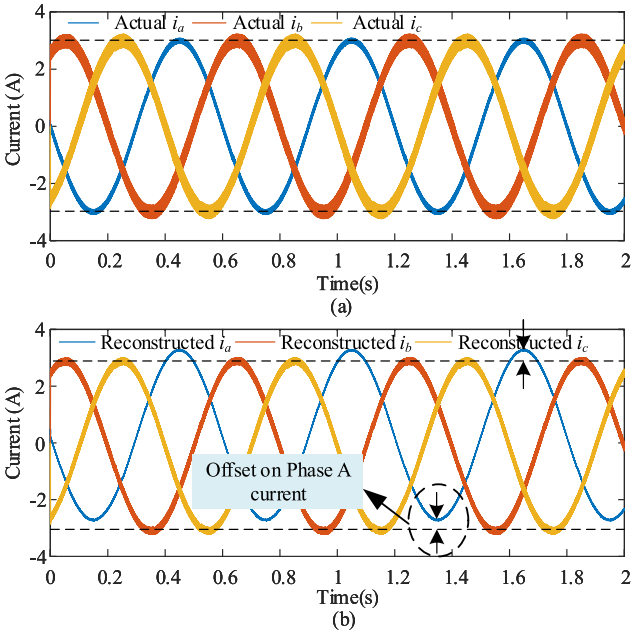

FIGURE 4. (a) Actual three-phase currents when injecting β-axis Square Wave in simulation, (b)simulated reconstructed three-phase currents.

The injection voltage can be expressed as:

$$\begin{bmatrix} v_{\alpha,h} \\ v_{\beta,h} \end{bmatrix} = V_h \begin{bmatrix} \cos(\omega_h t) \\ \sin(\omega_h t) \end{bmatrix} \tag{10}$$

where, $\omega_h = 2\pi f_{sw}/6$, and f_{sw} is the switching frequency.

The induced current is shown as:

$$\begin{bmatrix} i_{\alpha,h} \\ i_{\beta,h} \end{bmatrix} = \frac{V_h}{L^2 - \Delta L^2} \int \mathbf{L_h} \cdot \begin{bmatrix} \cos(\omega_h t) \\ \sin(\omega_h t) \end{bmatrix} dt \tag{11}$$

After simplifying,

$$\begin{bmatrix} i_{\alpha,h} \\ i_{\beta,h} \end{bmatrix} = A \begin{bmatrix} \frac{L}{\omega_h} \sin(\omega_h t) - \frac{\Delta L}{2\omega_e - \omega_h} \sin(2\theta_e - \omega_h t) \\ -\frac{L}{\omega_h} \cos(\omega_h t) + \frac{\Delta L}{2\omega_e - \omega_h} \cos(2\theta_e - \omega_h t) \end{bmatrix} \tag{12}$$

where,

$$A = \frac{V_h}{L^2 - \Delta L^2}$$

This six-direction injection method can be regarded as a six-step high frequency sinusoidal injection. Therefore, the position information can be extracted from the inducted current similar to the standard demodulation methods without the knowledge of the motor parameters. Due to the advantages of no parameter sensitivity and no offset on the current reconstruction, the six-direction injection method is preferred to be utilized at low-speed operation in this paper.

III. MODIFIED CURRENT RECONSTRUCTION FOR POSITION AND SPEED ESTIMATION WITH HF INJECTION

The proposed position sensorless control scheme for low-speed operation of IPMSMs takes advantage of the favourable high frequency signal to reconstruct the three-phase current and to estimate the position and speed by processing the current waveform. The entire system diagram is depicted in Fig. 7.

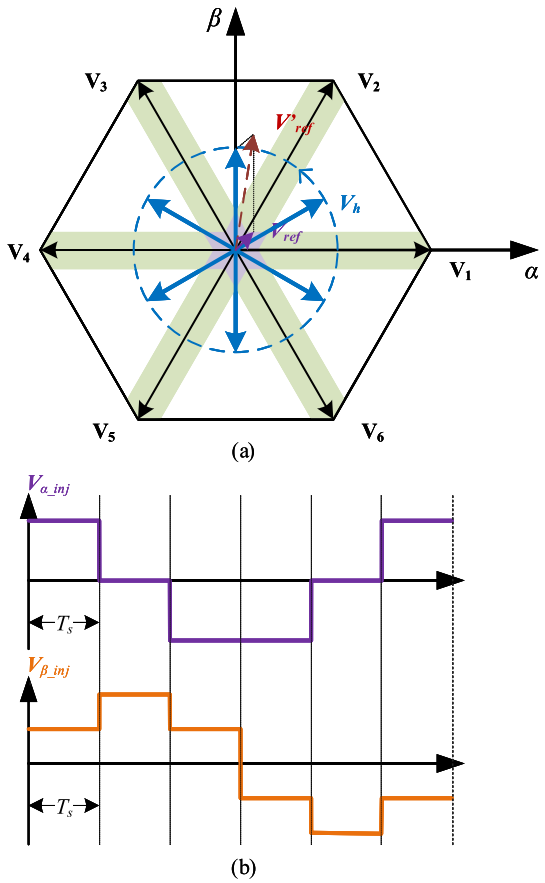

FIGURE 5. (a) Illustration of six-direction injection, (b) injection waveform in $\alpha - \beta$ frame.

A. POSITION AND SPEED ESTIMATION

The current process for the position and speed estimation is different according to the injection waveform, as shown in Fig. 6.

In the six-direction injection method, a high pass filter (HPF) is required to extract the induced current, whereas the induced current can be obtained from the difference between adjacent samples for β-axis injection method.

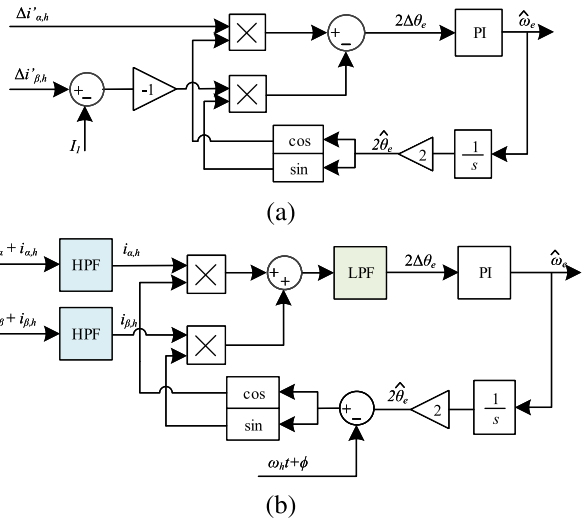

FIGURE 6. (a) Current processor of β-axis injection, (b) current processor of six direction injection.

In addition, the induced current contains the injection frequency.

The position extraction from the response currents is based on the following equations for the six direction injection method.

$$i_{\alpha,h}\cos(2\hat{\theta}_e - \omega_h t) - i_{\beta,h}\sin(2\hat{\theta}_e - \omega_h t) = A_1\sin(2\hat{\theta}_e - 2\omega_h t) + A_2\sin(2\hat{\theta}_e - 2\theta_e) \quad (13)$$

where,

$$A_1 = -A\frac{L}{\omega_h}, \quad A_2 = A\frac{\Delta L}{2\omega_e - \omega_h}$$

After a low pass filter (LPF), the first component can be eliminated and the equation will be approximately equal to $2A_2(\hat{\theta}_e - \theta_e)$. Therefore, the speed can be acquired by utilizing a PI regulator. Meanwhile, via integrating the speed, the position can be estimated.

Although it is more convenient to process the current without designing any filters for the β-axis injection method,

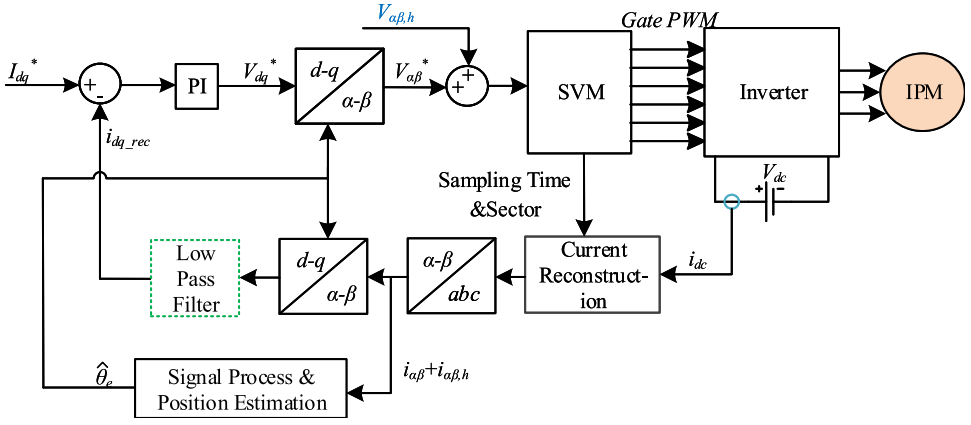

FIGURE 7. System diagram.

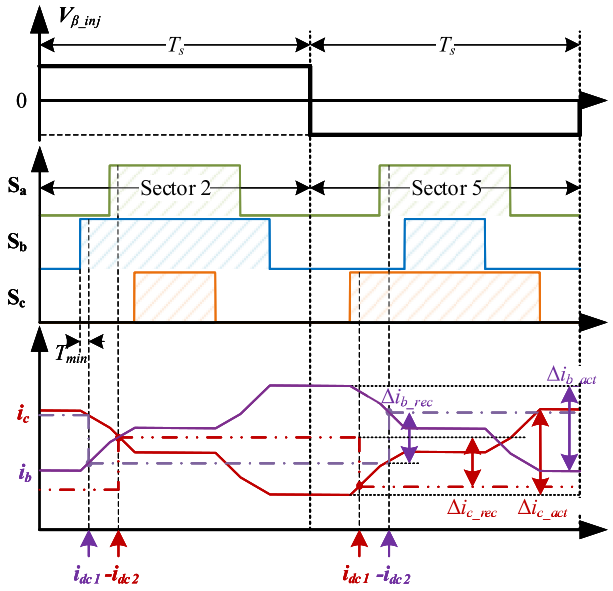

FIGURE 8. Switching state and phase current waveform when applying β-axis injection.

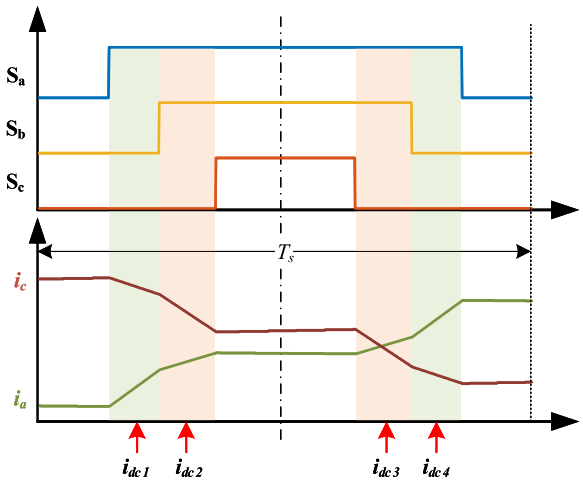

FIGURE 9. Current sampling of dc-link current sensor.

the performance is reliant on the motor parameters and the calibration of the current sensor. Six-direction injection method requires filters, but it eliminates the dependence on the parameters, and therefore results in accurate and reliable position estimation.

B. MODIFIED CURRENT RECONSTRUCTION METHOD

In the full sensors control, the three-phase currents are sampled simultaneously, whereas, in the reconstruction method, the dc links current is measured at different sampling instants for the three phase currents. This asynchronous reconstruction of phase currents influences the accuracy of the position estimation. A modified current reconstruction scheme is proposed in this paper for the purpose of improving the position estimation.

TABLE 2. Proposed three-phase current reconstruction method.

Sec	Phase A Current i_a	Phase B Current i_b	Phase C Current i_c
1	$(i_{dc1}+i_{dc4})/2$	$-(i_a+i_c)$	$-(i_{dc2}+i_{dc3})/2$
2	$-(i_b+i_c)$	$(i_{dc1}+i_{dc4})/2$	$-(i_{dc2}+i_{dc3})/2$
3	$-(i_{dc2}+i_{dc3})/2$	$(i_{dc1}+i_{dc4})/2$	$-(i_a+i_b)$
4	$-(i_{dc2}+i_{dc3})/2$	$-(i_a+i_c)$	$(i_{dc1}+i_{dc4})/2$
5	$-(i_b+i_c)$	$-(i_{dc2}+i_{dc3})/2$	$(i_{dc1}+i_{dc4})/2$
6	$(i_{dc1}+i_{dc4})/2$	$-(i_{dc2}+i_{dc3})/2$	$-(i_a+i_b)$

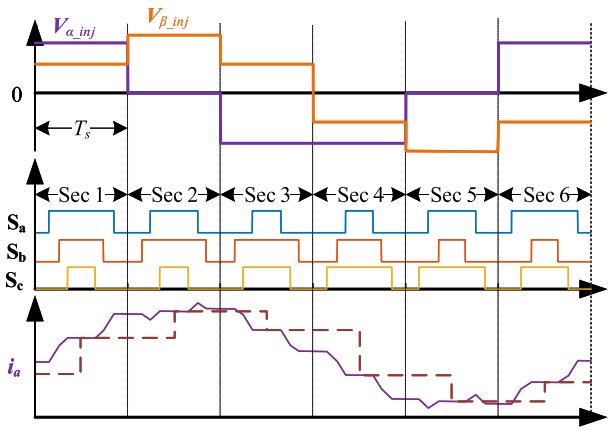

FIGURE 10. Switching state and phase current waveform when applying six direction injection.

The actual waveforms of Phase B and Phase C with β-axis injection are illustrated in Fig. 8. The current goes up and down periodically based on the injected voltage on β-axis. Traditionally, the current is sampled at the beginning of the PWM. In the conventional reconstruction method, the current measurement from dc-link current sensor is sampled at the interval of an effective voltage vector as shown in Fig. 8 with the sampled currents denoted as i_{dc1} and i_{dc2}. Shown as (8), $\Delta i_{\alpha,h}$ and $\Delta i_{\beta,h}$ contain the position information, so the current differences, which are denoted as Δi_{b_act} and Δi_{c_act} in Fig. 8, are also the key to estimate the precise position. However, the reconstructed current difference Δi_{b_rec} and Δi_{c_rec} have a reduction compared to the actual ones (Δi_{b_act} and Δi_{c_act}) as shown in Fig. 8, which can lead to non-negligible position estimation error.

In the modified current reconstruction method, the effect of unaligned (or asynchronous) sample timing is effectively reduced. According to seven-segment SVM, one identical effective voltage vector appears twice in one switching period. Thus, there are two timing intervals for the dc-link current sensor to capture one phase current. Therefore, in the modified current reconstruction method, the dc-link current is captured at two instants to identify one phase current in one switching period. So the total four instants corresponding to two phases are shown in Fig. 9. The average of the two instants effectively provides the corresponding phase current. In this way, the three-phase current measurement is aligned at the middle instant of the switching period. The new current

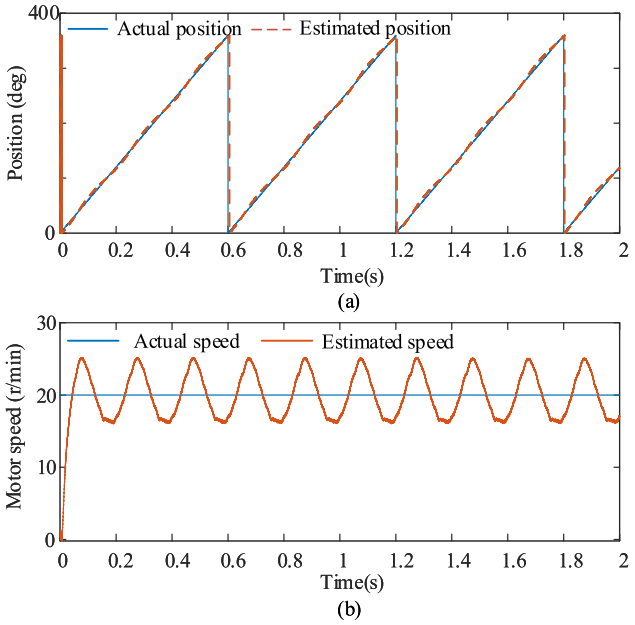

FIGURE 11. Simulation results of sensorless control with conventional current reconstruction.

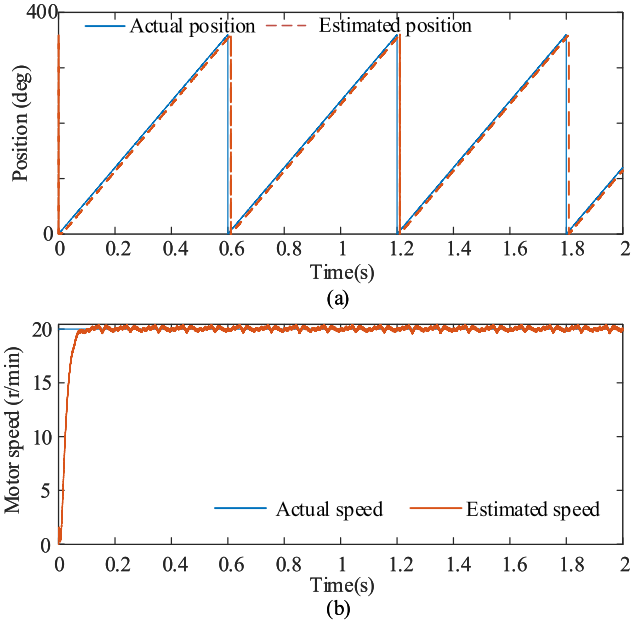

FIGURE 12. Simulation results of sensorless control with modified current reconstruction.

reconstruction method is presented in TABLE 2. It should be noted that the PWM waveform is kept symmetrical at all the time, unlike PWM modification based current reconstruction methods.

The modified method aligns the reconstructed phase current at the middle of the cycle as illustrated before for the β-axis injection. However, the improved reconstruction method cannot solve the other problems associated with β-axis injection, because the β-axis injection method requires

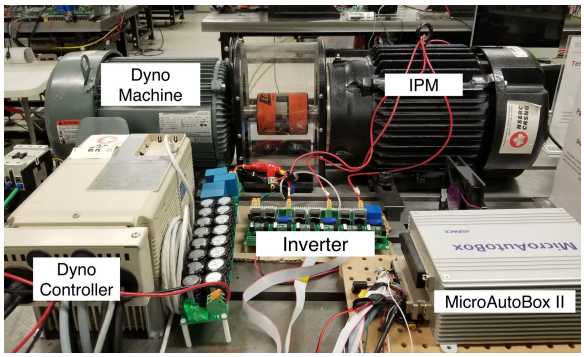

FIGURE 13. Experiment bench of IPMSM.

TABLE 3. Specification of IPMSM.

Parameter	Values	Parameter	Values
Rated current	9.4 A	Rated torque	29.7 Nm
Number of poles	10	d axis inductance	11 mH
q axis inductance	14.3 mH	Stator resistance	400 mΩ
PM flux linkage	333.3 mWb	DC link voltage	300 V

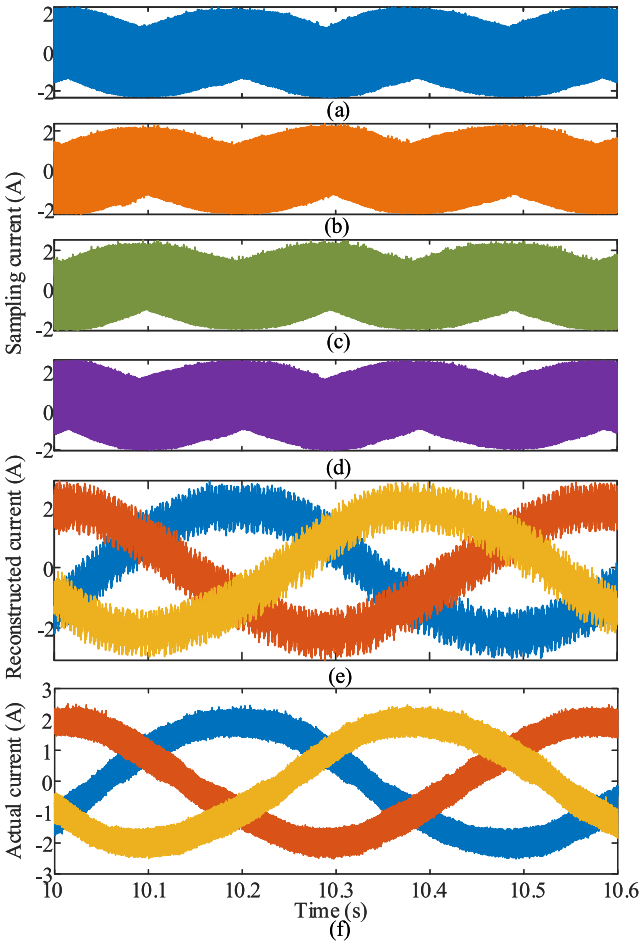

FIGURE 14. (a)-(d) Sample current from dc-link current sensor, (e) reconstructed phase current, (f) actual phase current.

to sample the current at the beginning of the switching period. Therefore, the benefits of the improved reconstruction

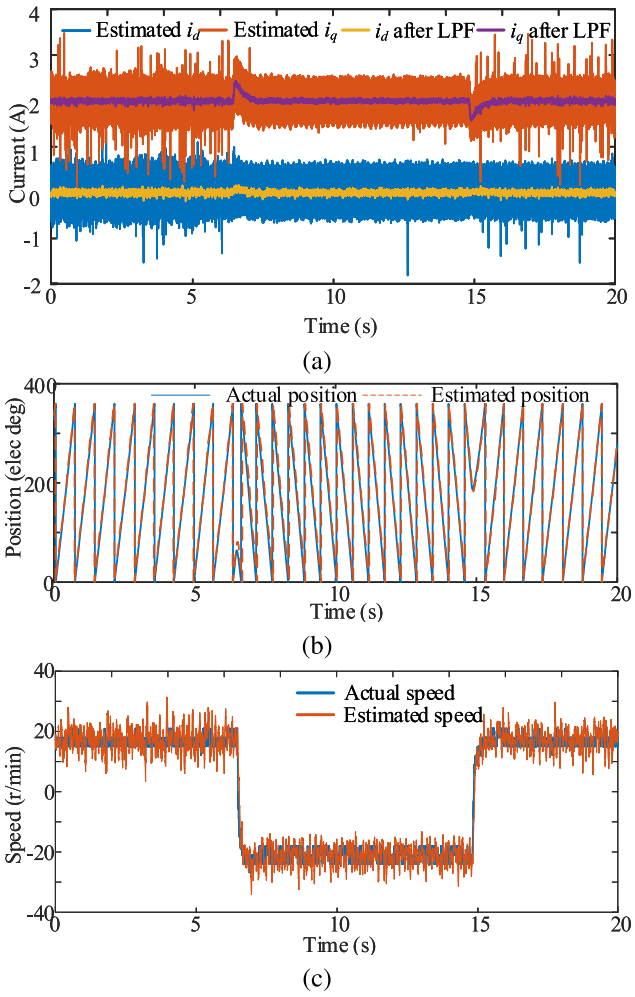

FIGURE 15. Experimental performance of changing speed (a) estimated $d-q$ axis current before and after LPF, (b) position comparison, (c) speed comparison.

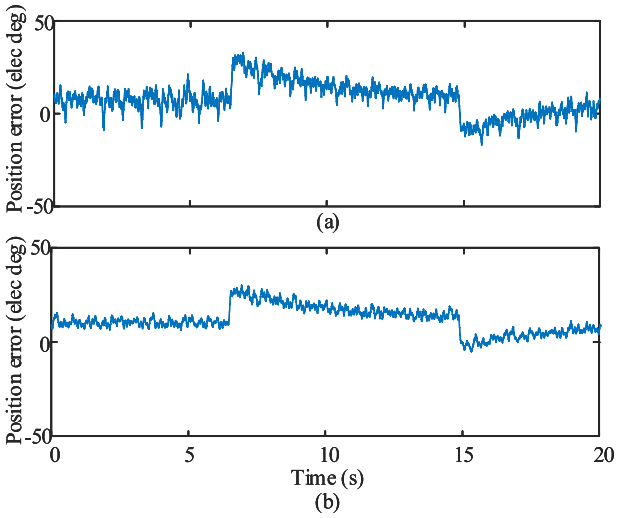

FIGURE 16. Experimental results of changing speed (a) error of position estimation by using reconstructed current, (b) error of position estimation by using actual current.

method on position estimation are analyzed for six-direction injection method in this paper. The Phase A current, switching states, and sampling instants for the six-direction injection method are shown in Fig. 10.

The improvement on position and speed estimations with the modified reconstruction method is obvious in Fig. 12 if compared to that of the conventional method in Fig. 11. The results in Fig. 12 and Fig. 11 are from simulation with six-direction square wave injection. The parameters used for the PLL in both cases are the same. In Fig. 11(a), there exists a fluctuation in the estimated position waveform. The estimated speed in Fig. 11(b) with the conventional reconstruction method contains a third-order harmonic oscillation, which has a magnitude of around 5 r/min. The tuning of the estimator parameters cannot eliminate this harmonic oscillation as it is mainly due to the unaligned measurements of three-phase currents. Thanks to the modified current reconstruction, the third-order harmonic is greatly reduced, as shown in Figure 12.

IV. EXPERIMENT VERIFICATION

The experiments are implemented in dSpace platform for a 5 kW IPMSM. The switching devices for the VSI are MOSFETs and the switching frequency is fixed to 10 kHz. The test bench for the experiments is demonstrated in Fig. 13. The motor specification is shown in TABLE 3. The dyno machine used in this test is a 5 kW induction machine, which is controlled by Yaskawa drive. According to the algorithm introduced previously, there are four triggered threads applied in one control period to sample and acquire the dc-link current. The three phase current is reconstructed according to the relationship between the dc-link current and the active voltage vector. The main program calculates the estimated position from the reconstructed current and feeds back the current and position to control the IPMSM machine.

In the experiment verification, the speed is controlled by the dyno machine. The currents of IPMSM are controlled by standard PI regulators. Three phase-current sensors and a position sensor are installed for the comparison. The amplitude of the injected signal is 70 V in the experiments. The selection of the amplitude may vary with the applied speed and torque to guarantee the reference voltage in the measurable region.

A. CURRENT RECONSTRUCTION PERFORMANCE

Fig. 14(a)-(d) shows the sampled current from the dc-link current sensor when i_q is controlled at 2 A. It is observed that the first and the fourth sample currents have the same shape because the current is sampled at the same corresponding voltage vector interval, which is also true for the second and the third ones. Through comparing the reconstructed current with the actual value, the immeasurable region of dc-link current measurement is avoided thanks to the six-direction square wave injection.

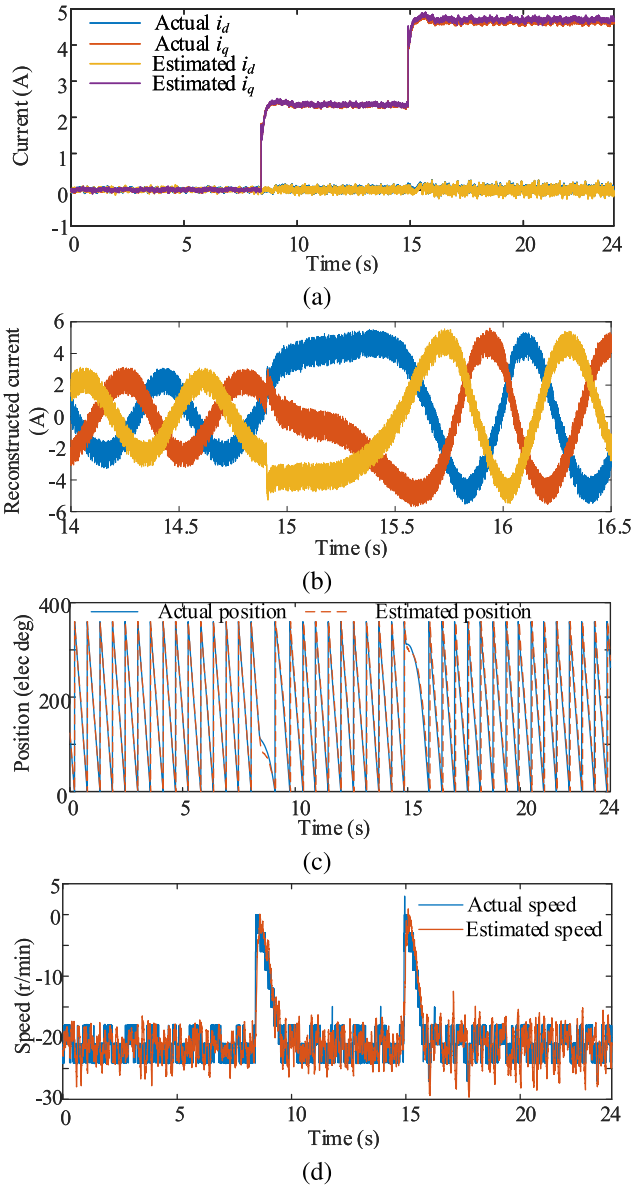

FIGURE 17. Experimental results of changing current (a) $d-q$ axis current comparison, (b) reconstructed phase current during transient process, (c) position comparison, (d) speed comparison.

B. SPEED TRANSIENT PERFORMANCE OF LOW SPEED SENSORLESS CONTROL

The speed transient test is conducted by applying step speed between 20 r/min and -20 r/min with 20% load. The performance is presented in Fig. 15. The $d-q$ axes currents are controlled to constant values during the speed transient process. With the function of the LPF, the noise in the estimated currents caused by noise from the dc-link current measurement is eliminated, as shown in Fig. 15(a). It should be noted that the filtered reconstructed current is used as the feedback to the current controller to avoid oscillation in reference voltage. The oscillation in reference voltage adversely affects the reconstruction and estimation of position and speed. Thanks to the PLL, the

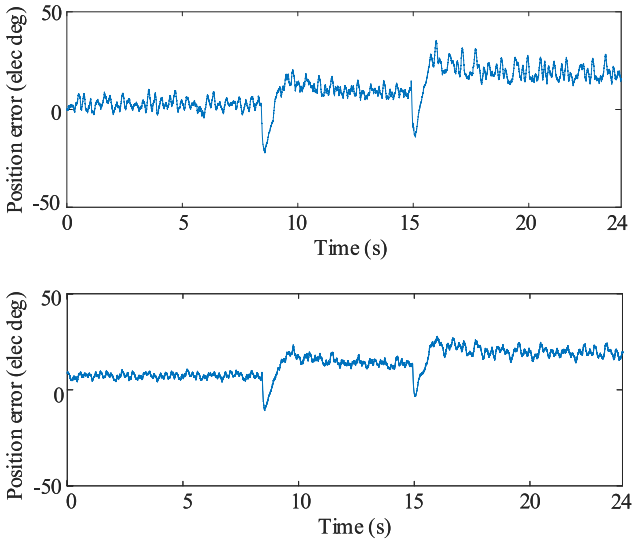

FIGURE 18. Experimental results of changing current (a) error of position estimation by using reconstructed current, (b) error of position estimation by using actual current.

estimated position and speed can track the actual values with the rapid response as in Fig. 15(b)-(c). The position error between the estimated position and the actual one is presented in Fig. 16(a). The steady-state error is around 10 electrical degree. Fig. 16(b) shows the position error of the estimated position by using actual current, which has almost the same value as that in Fig. 16(a) when the speed changes. This result explains that the steady-state error comes from the sensorless control due to the function of LPF and time delay when implementing this method in practice. It proves the sensorless performance with the dc-link current sensor is comparable with that with full current sensors.

C. TORQUE TRANSIENT PERFORMANCE OF LOW SPEED SENSORLESS CONTROL

Torque transient performance is validated through a test conducted by rotating the motor at a negative speed, which is -20 r/min. The load changes from 0 to 25% and from 25% to 50%. The experimental results are shown in Fig. 17. Through the comparison between the actual current and estimated $d-q$ currents in Fig. 17(a), and the reconstructed phase current in Fig. 17(b), it can be observed that, the transient process is stable without any deviation. The position comparison and the speed comparison with the actual values are also given in Fig. 17(c)-(d). The position error in Fig. 18 shows that the accuracy of the estimation becomes worse with the increase of load. However, compared to the position estimated by the actual phase current, the estimation performance is similar.

V. CONCLUSION

This paper proposes a high frequency injection method to deal with the immeasurable region for low-speed sensorless control of IPMSMs with a single dc-link current sensor. Two possible injection methods without shifting the PWM

waveform are introduced and analyzed theoretically, and six-direction injection method is adopted in this paper. The reconstruction of the phase current is completed by detecting the dc-link current at different sample instants according to the standard method, but that deteriorates the performance of position estimation. As a solution, the dc-link current is captured four times every switching period to reconstruct the three phase currents at the middle instant of a switching period. The low-speed sensorless control with a single dc-link current sensor is realized is implemented in dSpace platform for experimental validation. The dynamic performance of changing speed and changing current is provided in the experimental results to prove that the method is comparable with the low-speed sensorless control with full current sensors.

REFERENCES

[1] D. Xu, B. Wang, G. Zhang, G. Wang, and Y. Yu, "A review of sensorless control methods for AC motor drives," *CES Trans. Elect. Mach. Syst.*, vol. 2, no. 1, pp. 104–115, 2018.

[2] Y. Zhao, C. Wei, Z. Zhang, and W. Qiao, "A review on position/speed sensorless control for permanent-magnet synchronous machine-based wind energy conversion systems," *IEEE J. Emerg. Sel. Topics Power Electron.*, vol. 1, no. 4, pp. 203–216, Dec. 2013.

[3] Y. Sun, M. Preindl, S. Sirouspour, and A. Emadi, "Unified wide-speed sensorless scheme using nonlinear optimization for IPMSM drives," *IEEE Trans. Power Electron.*, vol. 32, no. 8, pp. 6308–6322, Aug. 2017.

[4] S. Nalakath, Y. Sun, M. Preindl, and A. Emadi, "Optimization-based position sensorless finite control set model predictive control for IPMSMs," *IEEE Trans. Power Electron.*, vol. 33, no. 10, pp. 8672–8682, Oct. 2018.

[5] Z. Chen, M. Tomita, S. Doki, and S. Okuma, "An extended electromotive force model for sensorless control of interior permanent-magnet synchronous motors," *IEEE Trans. Ind. Electron.*, vol. 50, no. 2, pp. 288–295, Apr. 2003.

[6] F. Genduso, R. Miceli, C. Rando, and G. R. Galluzzo, "Back EMF sensorless-control algorithm for high-dynamic performance PMSM," *IEEE Trans. Ind. Electron.*, vol. 57, no. 6, pp. 2092–2100, Jun. 2010.

[7] G. Wang, D. Xiao, G. Zhang, C. Li, X. Zhang, and D. Xu, "Sensorless control scheme of IPMSMs using HF orthogonal square-wave voltage injection into a stationary reference frame," *IEEE Trans. Power Electron.*, vol. 34, no. 3, pp. 2573–2584, Jun. 2019.

[8] Y. Xu, H. Yan, J. Zou, B. Wang, and Y. Li, "Zero voltage vector sampling method for PMSM three-phase current reconstruction using single current sensor," *IEEE Trans. Power Electron.*, vol. 32, no. 5, pp. 3797–3807, Jul. 2017.

[9] Y. Cho, T. Labella, and J. S. Lai, "A three-phase current reconstruction strategy with online current offset compensation using a single current sensor," *IEEE Trans. Ind. Electron.*, vol. 59, no. 7, pp. 2924–2933, 2012.

[10] M. Carpaneto, P. Fazio, M. Marchesoni, and G. Parodi, "Dynamic performance evaluation of sensorless permanent-magnet synchronous motor drives with reduced current sensors," *IEEE Trans. Ind. Electron.*, vol. 59, no. 12, pp. 4579–4589, Dec. 2012.

[11] J. H. Im, S. I. Kim, and R. Y. Kim, "An improved saliency-based sensorless drive with single current sensor using current prediction method for permanent-magnet synchronous motors," in *Proc. IEEE Veh. Power Propuls. Conf.*, Oct. 2016, pp. 1–6.

[12] I. Aminoroaya and S. Vaez-Zadeh, "Permanent magnet synchronous motor control using DC-link current regulation," in *Proc. Ind. Electron. Conf. (IECON)*, Oct. 2016, pp. 7077–7082.

[13] K. S. Kim, H. B. Yeom, H. K. Ku, J. M. Kim, and W. S. Im, "Current reconstruction method with single DC-link current sensor based on the PWM inverter and AC motor," in *Proc. IEEE Energy Convers. Congr. Expo. (ECCE)*, no. 1, Sep. 2014, pp. 250–256.

[14] B. Saritha and P. A. Janakiraman, "Sinusoidal three-phase current reconstruction and control using a DC-link current sensor and a curve-fitting observer," *IEEE Trans. Ind. Electron.*, vol. 54, no. 5, pp. 2657–2664, Oct. 2007.

[15] T. M. Wolbank and P. E. Macheiner, "Current-controller with single DC link current measurement for inverter-fed AC machines based on an improved observer-structure," *IEEE Trans. Power Electron.*, vol. 19, no. 6, pp. 1562–1567, Nov. 2004.

[16] B. Hafez, A. S. Abdel-Khalik, A. M. Massoud, S. Ahmed, and R. D. Lorenz, "Single-sensor-based three-phase permanent-magnet synchronous motor drive system with Luenberger observers for motor line current reconstruction," *IEEE Trans. Ind. Appl.*, vol. 50, no. 4, pp. 2602–2613, Jan. 2014.

[17] Y. Gu, F. Ni, D. Yang, and H. Liu, "Switching-state phase shift method for three-phase-current reconstruction with a single DC-link current sensor," *IEEE Trans. Ind. Electron.*, vol. 58, no. 11, pp. 5186–5194, Mar. 2011.

[18] H. Kim and T. M. Jahns, "Phase current reconstruction for AC motor drives using a DC link single current sensor and measurement voltage vectors," *IEEE Trans. Power Electron.*, vol. 21, no. 5, pp. 1413–1419, Sep. 2006.

[19] H. Kim and T. M. Jahns, "Current control for AC motor drives using a single DC-link current sensor and measurement voltage vectors," *IEEE Trans. Ind. Appl.*, vol. 42, no. 6, pp. 1539–1547, Nov. 2006.

[20] S. C. Yang, "Saliency-based position estimation of permanent-magnet synchronous machines using square-wave voltage injection with a single current sensor," *IEEE Trans. Ind. Appl.*, vol. 51, no. 2, pp. 1561–1571, Sep. 2015.

[21] J.-H. Im and R.-Y. Kim, "Improved saliency-based position sensorless control of interior permanent-magnet synchronous machines with single DC-link current sensor using current prediction method," *IEEE Trans. Ind. Electron.*, vol. 65, no. 7, pp. 5335–5343, Nov. 2018.

JING ZHAO received the B.E. and M.E. degrees in electrical engineering from Beihang University, Beijing, China, in 2011 and 2014, respectively. From 2014 to 2016, she was an Engineer with the Institution of Remote Sensing Equipment, Beijing. From 2016 to 2017, she was an Embedded Engineer with AheadX Tech Company Ltd., Beijing. Since September 2017, she has been a master student with a Research Team, McMaster Automotive Resource Center, McMaster University, Hamilton, ON, Canada. Her research interests include motor control and parameter estimation applied in electric and hybrid vehicle application.

SHAMSUDDEEN NALAKATH (S'07–M'11) received the M.S. degree in electrical engineering from the Indian Institute of Technology, Madras, India, in 2010, and the Ph.D. degree in electrical engineering from McMaster University, Hamilton, ON, Canada, in 2018.

Since 2018, he has been the Principal Research Engineer with the McMaster Automotive Resource Center, McMaster University, where he leads industrial research projects on electric motor controls and inverters for automotive applications. From 2010 to 2014, he was with the Advanced Engineering Group, M/s TVS Motor Company Ltd., India, where he worked in design and development of advanced electric machines for electric and hybrid vehicles. His main research interests include electric motor control, electric motor design, and power electronics for high-performance automotive traction applications.

ALI EMADI (S'98–M'00–SM'03–F'13) received the B.S. and M.S. degrees (Hons.) from the Sharif University of Technology, Tehran, Iran, in 1995 and 1997, respectively, and the Ph.D. degree from Texas A&M University, College Station, TX, USA, in 2000, all in electrical engineering. He was the Harris Perlstein Endowed Chair Professor of engineering and the Director of the Electric Power and Power Electronics Center and Grainger Laboratories, Illinois Institute of Technology, Chicago, IL, USA, where he established research and teaching facilities, as well as courses in power electronics, motor drives, and vehicular power systems. He was the Founder, the Chairman, and the President of Hybrid Electric Vehicle Technologies, Inc., (HEVT), a university spin-off company of Illinois Tech. He is currently the Canada Excellence Research Chair Laureate of McMaster University, Hamilton, ON, Canada. He holds the NSERC/FCA Industrial Research Chair in Electrified Powertrains and the Tier I Canada Research Chair of Transportation Electrification and Smart Mobility. He is also the principal author or coauthor of more than 450 journal and conference articles as well as several books, including *Vehicular Electric Power Systems* (2003), *Energy-Efficient Electric Motors* (2004), *Uninterruptible Power Supplies and Active Filters* (2004), *Modern Electric, Hybrid Electric, and Fuel Cell Vehicles* (Second Edition, 2009), and *Integrated Power Electronic Converters and Digital Control* (2009). He was a recipient of numerous awards and recognitions including the GM Best Engineered Hybrid System Award at Illinois Tech and McMaster University, in 2010, 2013, and 2015 competitions. He was an Advisor for the Formula Hybrid Teams at Illinois Tech and McMaster University. He was the Inaugural General Chair of the 2012 IEEE Transportation Electrification Conference and Expo (ITEC). He has chaired the several IEEE and SAE conferences in the areas of vehicle power and propulsion. He is an Editor of the *Handbook of Automotive Power Electronics and Motor Drives* (2005) and *Advanced Electric Drive Vehicles* (2014). He is also a Co-Editor of the *Switched Reluctance Motor Drives* (2018). He is also the founding Editor-in-Chief of the IEEE TRANSACTIONS ON TRANSPORTATION ELECTRIFICATION.